Results from the Relativistic Heavy Ion Collider

Bedangadas Mohanty*
Variable Energy Cyclotron Centre, Kolkata - 700064, INDIA

Selected results from the experimental program at the Relativistic Heavy Ion Collider (RHIC) facility at Brookhaven national laboratory are presented. These include measurements related to jet quenching, partonic collectivity, QCD critical point search and antimatter production.

1. Introduction

One of the main goals of the high energy heavy-ion collision program at the RHIC facility in Brookhaven National Laboratory is to study the Quantum chromodynamics (QCD) phase diagram [1, 2]. The QCD phase diagram is usually plotted as temperature (T) versus the chemical potential associated with the conserved baryon number ($\mu_{\rm B}$). Two fundamental properties of QCD, related to confinement and chiral symmetry, allows for two corresponding phase transitions when T and $\mu_{\rm B}$ are varied. Theoretically the phase diagram is explored through non-perturbative QCD calculations on lattice. The energy scale for the phase diagram ($\Lambda_{\rm QCD} \sim 200$ MeV and critical temperature, $T_C \sim 175$ MeV [2]) is such that it can be explored experimentally by colliding nuclei at varying beam energies in the laboratory.

The observations from the RHIC experiments (currently operational detectors are: PHENIX and STAR [3]) have clearly established the formation of a matter where the relevant degrees of freedom are quarks and gluons for Au+Au collisions at center of mass energy of 200 GeV per nucleon. In this paper we briefly review some of these results which includes the suppression of the high transverse momentum hadron production in Au+Au collisions relative to p+p collisions and the number of constituent quark scaling of elliptic flow of identified hadrons. In addition to these first observations in the field of heavy-ion collisions, STAR experiment at RHIC has recently reported the discovery of two new anti-matter nuclei, anti-hypertriton and anti-helium-4. The significance of these new observations, which were recently published in Science [4] and Nature [5] respectively, to the field of nuclear physics and cosmology are discussed. Following these discoveries at RHIC, the scientific program was extended to explore the QCD phase boundary and search for the signatures of the QCD critical point. For this, RHIC undertook a dedicated Beam Energy Scan program in year 2010-2011, where the colliding energy was varied between 7.7 and 200 GeV per nucleon. We present some selected new results from RHIC experiments from this scientific program.

2. Jet quenching and formation of a highly opaque medium

One of the most exciting results to date at RHIC is the discovery of suppression in the production of high transverse momentum (p_T) mesons in nucleus-nucleus collisions compared to corresponding data from the binary collision scaled p+p collisions [6]. This has been interpreted in terms of energy loss of partons in quark gluon plasma (QGP). This phenomena is called as the jet quenching in a dense partonic matter [7]. The energy loss by energetic partons traversing the dense medium formed in high-energy heavy-ion collisions is predicted to be proportional to both the initial gluon density [8] and the lifetime of the dense matter [9]. The results on high-p_T suppression are usually presented in terms of the nuclear modification factor (R_{AA}), defined as:

$$R_{AA}(p_{\rm T}) = \frac{dN_{AA}/d\eta d^2p_T}{T_{AB} d\sigma_{NN}/d\eta d^2p_T} \qquad (1)$$

*Electronic address: bmohanty@vecc.gov.in

where the overlap integral $T_{AB} = N_{binary}/\sigma_{NN}^{pp}$. N_{binary} is the number of binary collisions commonly estimated from Glauber model calculation [10], σ_{NN}^{pp} is the inelastic nucleon-nucleon cross section, N_{AA} is the yield in nucleus-nucleus collisions and η is the pseudorapidity.

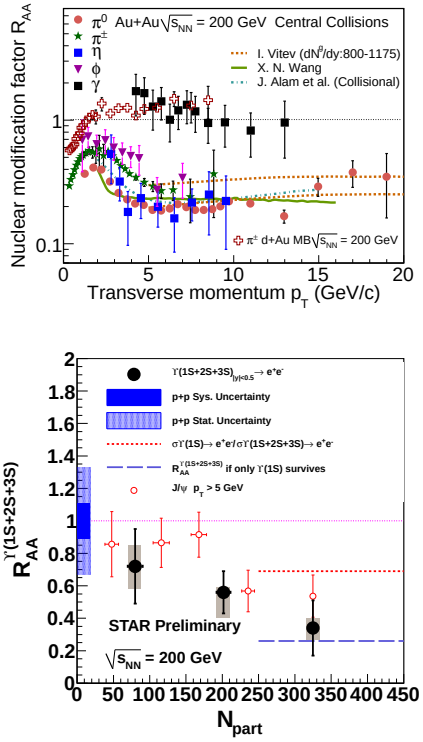

FIG. 1: Top panel: Compilation of the nuclear modification factor ($R_{\rm AA}$) for mesons and direct photons as measured in RHIC experiments at midrapidity for central Au+Au collisions at $\sqrt{s_{\rm NN}}$ = 200 GeV. Also shown are the $R_{\rm dAu}$ for charged pions for $\sqrt{s_{\rm NN}}$ = 200 GeV. The lines are results from various model calculations. See text for more details. Bottom panel: Υ(1S+2S+3S) R_{AA} as a function of N_{part} compared to the J/ψ R_{AA} for $p_T > 5$ GeV/c in Au + Au collisions at $\sqrt{s_{NN}} = 200$ GeV. The shaded bands at $N_{part} = 0$ represent statistical and systematic uncertainties in p + p measurements.

In Fig. 1 top panel we show the RHIC data for the $R_{AA}(p_{\rm T})$, for various produced mesons [11] and direct photons [12] in central Au+Au collisions at midrapidity. A large suppression in high $p_{\rm T}$ meson production is observed, and those for π^0's being almost flat at $R_{AA} \simeq 0.2$ up to 20 GeV/c. The figure also shows that the level of suppression for π^0's, η's and ϕ-mesons are very similar, which supports the conclusion that the suppression occurs in the partonic phase, not in the hadronic phase. This strong suppression of meson production is in contrast to the behavior of direct photons, also shown in the figure. The direct photons follow binary scaling (i.e. $R_{AA} \simeq 1$) or no suppression. This is a strong evidence that the suppression is not an initial state effect, but a final state effect caused by the high density medium with color charges created in the collision. This is further consolidated by a demonstration through a controlled experiment using deuteron on Au ion collisions, which gave a $R_{dAu}(p_{\rm T}) \sim 1$ for $\pi^{\pm}$ at midrapidity and high $p_{\rm T}$ [13].

The various curves in the Fig. 1 represents different model calculations. The dashed curve shows a theoretical prediction using the GLV parton energy loss model [8] . The model assumes an initial parton density $dN/dy = 800 - 1175$, which corresponds to an energy density of approximately 5-15 GeV/fm^3. The lower dashed curves are for higher gluon density. The precision high $p_{\rm T}$ data at RHIC has been used to characterize medium density fairly accurately. The conclusion being that the medium formed in central Au+Au collisions at RHIC has a high degree of opacity [14]. In addition, theoretical studies suggest that for a given initial density, the $R_{AA}(p_{\rm T})$ values are also sensitive to the lifetime (τ) of dense matter formed in heavy-ion collisions [9]. The solid curves are predictions from Ref. [9] at $\sqrt{s_{\rm NN}} = 200$ GeV with $\tau = 10$ fm/c (i.e. larger than the typical system size of $\sim$ 6-7 fm). The parton energy loss calculations discussed above attributes the opacity to plasma induced radiation of gluons, much like ordinary bremsstrahlung of photons by electrons. However, the quantitatively large suppression pattern observed at high $p_{\rm T}$, for both light hadrons and those involving heavy

quarks [15], showed that the mechanism of energy loss is far from being a settled issue, namely, the relative contribution of radiative and collisional forms. As an example, shown in Fig. 1 is a comparison of the data to theoretical results (dot-dash curves) on R_{AA} from models that consider only collisional energy loss [16]. This model gives R_{AA} values at high $p_{\rm T}$ close to the measured values and similar to corresponding values from models having only a radiative mechanism for parton energy loss.

The suppression of J/ψ and Υ due to color screening of $c\bar{c}$ pairs is expected to be one of the unambiguous signature of QGP formation. Calculations constrained by lattice data indicates that at 200 GeV $\Upsilon(3S)$ state should be completely dissociated, while $\Upsilon(2S)$ state may dissociate and $\Upsilon(1S)$ state should survive. Studying nuclear modification factor for Υ could constrain the QGP temperature. Figure 1 bottom panel shows the R_{AA} for high p_T J/ψ ($p_T > 5$ GeV/c) and Υ(1S+2S+3S) as a function of number of participants N_{part} in Au + Au collisions at $\sqrt{s_{NN}} = 200$ GeV. The high p_T J/ψ shows suppression in central collisions. The Υ(1S+2S+3S) R_{AA} shows similar suppression pattern as high p_T J/ψ.

3. Partonic collectivity and fluid with low viscosity

Elliptic flow, v_2, is an observable which is thought to reflect the conditions from the early stage of the collisions [17]. In non-central heavy-ion collisions, the initial spatial anisotropy of the overlap region of the colliding nuclei is transformed into an anisotropy in momentum space through interactions between the particles. As the system expands it becomes more spherical, thus the driving force quenches itself. Therefore the elliptic flow is sensitive to the collision dynamics in the early stages. It is measured, by calculating $\langle\cos(2(\phi - \Psi))\rangle$, where ϕ is the azimuthal angle of the produced particles and Ψ is the azimuthal angle of the impact parameter, and angular brackets denote an average over many particles and events.

Figure 2 top panel shows the elliptic flow v_2 plotted versus transverse kinetic energy

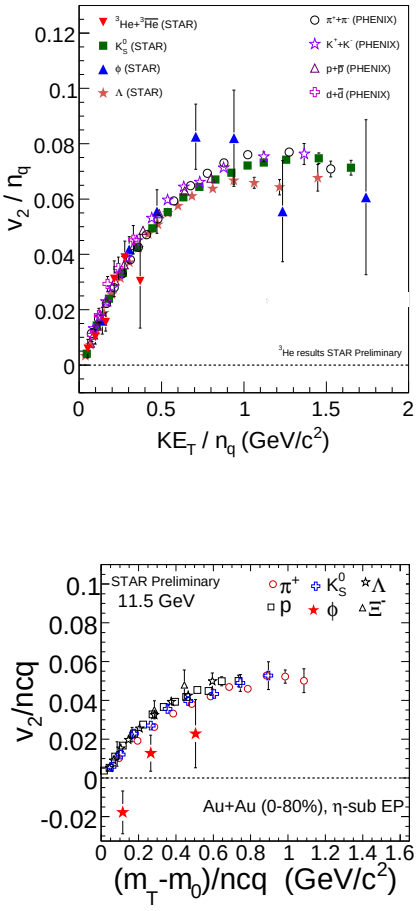

FIG. 2: Top panel: Compilation of the number of constituent quark scaled v_2 as a function of the scaled transverse kinetic energy. The data is from Au+Au collisions at midrapidity for $\sqrt{s_{\rm NN}} = 200$ GeV. Bottom panel: v_2/ncq vs. $(m_{\rm T} - m_0)$/ncq for 0-80% Au+Au collisions at 11.5 GeV.

$(m_{\rm T} - m_0)$, both divided by the number of constituent quarks. Where $m_{\rm T}$ is the transverse mass of a hadron with mass m_0. The v_2 for all identified hadrons as well as light nuclei below $(m_{\rm T} - m_0) \sim 1$ GeV/c^2 falls on a universal curve [24]. This first such observation of scaling behavior in v_2 in heavy-ion collisions provides the evidence for the forma-

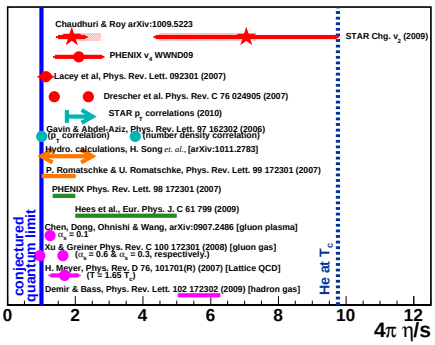

FIG. 3: Compilation of η/s extracted from various measurements in heavy-ion collisions at RHIC.

tion of a partonic matter and development of substantial amount of collectivity in partonic phase during the Au + Au collision process at 200 GeV. It is very hard to explain this observed pattern in a scenario where only hadronic matter exists throughout the interaction, whereas the hypothesis of coalescence of hadrons from de-confined quarks offers a ready explanation [23]. Turn-off of the scaling at a given beam energy would indicate the hadronic side of the phase boundary. Figure 2 bottom panel shows similar results as the top panel but for 11.5 GeV collisions. We observe that ϕ-meson v_2 drops off the common trend followed by other particles. The interaction of ϕ-mesons with nucleons are expected to be smaller compared to other hadrons and at top RHIC energy it was observed that ϕ-mesons freeze-out close to the transition temperature predicted by lattice QCD [25]. All these make ϕ-meson a carrier of early stage information in heavy-ion collisions. ϕ-meson v_2 was found to follow the ncq scaling at top RHIC energy and this was used to conclude that a substantial amount of collectivity at 200 GeV has been developed at the partonic stage. Small ϕ-meson v_2 at 11.5 GeV would then indicate collectivity contribution from partonic interactions to decrease with decrease in beam energy [25].

The v_2 measurements of light quark carrying hadrons, the nuclear modification factor and v_2 for heavy quark carrying hadrons and the differential $p_{\rm T}$ correlations for charged hadrons have been used to extract information of a dimensionless ratio, shear viscosity to entropy (η/s), for the medium formed in heavy-ion collisions at RHIC [26]. Figure 3 shows the compilation of η/s extracted from various measurements [27]. It is observed to lie between the lowest η/s ($\sim 1/4\pi$) bound conjectured from the gauge-gravity duality (or the AdS/CFT correspondence) [28] and those for liquid Helium at T_c [29]. A low value of η (η/s within a factor 1-10 of the quantum limit) indicates that the matter formed in heavy-ion collisions at RHIC has low viscosity, hence is a strongly coupled system. However it must be kept in mind that the η/s values extracted are highly model dependent and may involve assumptions which are not yet fully tested. Most of the results involves comparison of v_2 to viscous hydrodynamic calculations which are still in early stage of development or transport model inspired fits to the data [30].

4. QCD critical point and phase transition temperature

The critical point (CP) is a landmark point in the QCD phase diagram, observation of which will make the QCD phase diagram a reality. A close collaboration between the experiments and theory perhaps will lead to its discovery. The first step in this process is to establish an observable for CP which can be measured experimentally and can be related to QCD calculations. In this context, it is important to recall that for a static, infinite medium, the correlation length (ξ) diverges at the CP. ξ is related to various moments of the distributions of conserved quantities such as net-baryons, net-charge, and net-strangeness [31]. Typically variances ($\sigma^2 \equiv \langle(\Delta N)^2\rangle$; $\Delta N = N - M$; M is the mean) of these distributions are related to ξ as $\sigma^2 \sim \xi^2$ [32]. Finite size and time effects in heavy-ion collisions put constraints on the values of ξ. A theoretical calculation suggests $\xi \approx$ 2-3 fm for heavy-ion collisions [33]. It was recently shown that higher moments of distributions of conserved quantities, measuring deviations

from a Gaussian, have a sensitivity to CP fluctuations that is better than that of σ^2, due to a stronger dependence on ξ [34]. The numerators in skewness ($S = \langle(\Delta N)^3\rangle / \sigma^3$) goes as $\xi^{4.5}$ and kurtosis ($\kappa = [\langle(\Delta N)^4\rangle / \sigma^4]$ - 3) goes as ξ^7. A crossing of the phase boundary can manifest itself by a change of sign of S as a function of energy density [34, 35].

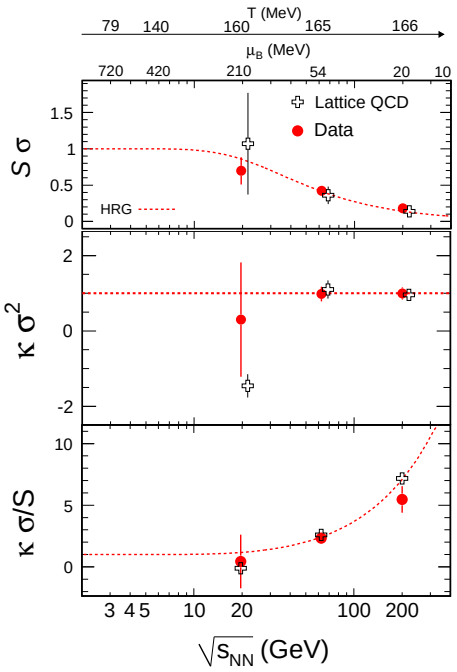

FIG. 4: (Color online) $\sqrt{s_{\rm NN}}$ dependence of $S\sigma$, $\kappa\sigma^2$ and $\frac{\kappa\sigma}{S}$ for net-proton distributions measured at RHIC [36]. The results are compared Lattice QCD calculations [37] and HRG model [38]. Also shown on the top are the temperature and baryon chemical potential values at chemical freeze-out extracted from particle yields using a thermal model.

The first connections between QCD calculations and experiment has been recently made [2, 36]. Lattice calculations and QCD-based models show that moments of net-baryon distributions are related to baryon number ($\Delta N_{\rm B}$) susceptibilities ($\chi_{\rm B} = \frac{\langle(\Delta N_{\rm B})^2\rangle}{VT}$; V is the volume) [37, 39]. Then one can construct ratios such as:

$$S\sigma = \frac{T\chi_B^{(3)}}{\chi_B^{(2)}}, \kappa\sigma^2 = \frac{T^2\chi_B^{(4)}}{\chi_B^{(2)}} \quad \text{and} \quad \frac{\kappa\sigma}{S} = \frac{T\chi_B^{(4)}}{\chi_B^{(3)}},$$

which do not contain the volume and therefore provide a direct and convenient comparison of experiment and theory. In the above expressions the left hand side of each equality can be measured in an experiment whereas the right hand side can be calculated by lattice QCD. Close to the CP models predict the $\Delta N_{\rm B}$ distributions to be non-Gaussian and susceptibilities to diverge causing the experimental observables to have large values. The experimental values should also be compared to those expected from statistics, for example if the p and $\bar{p}$ distributions are individually Poissonian then $\kappa\sigma^2$ for net-protons is unity.

Experimentally measuring event-by-event net-baryon number is difficult. However, the net-proton multiplicity ($N_{\rm p} - N_{\bar{\rm p}} = \Delta N_{\rm p}$) distribution is measurable. Theoretical calculations have shown that $\Delta N_{\rm p}$ fluctuations reflect the singularity of the charge and baryon number susceptibility as expected at the CP [40]. Non-CP model calculations show that the inclusion of other baryons does not add to the sensitivity of the observable [36].

Figure 4 shows the energy dependence of $S\sigma$, $\kappa\sigma^2$ and $\frac{\kappa\sigma}{S}$ for $\Delta N_{\rm p}$, compared to lattice QCD [37] and Hadron Resonance Gas (HRG) model which does not include a CP [38]. The experimental values plotted are for central Au+Au collisions for $\sqrt{s_{\rm NN}}$ = 19.6, 62.4 and 200 GeV. The lattice calculations, which predict a CP around $\mu_{\rm B} \sim 300$ MeV, are carried out using two-flavor QCD with number of lattice sites in imaginary time to be 6 and mass of pion around 230 MeV [37]. The ratios of the non-linear susceptibilities at finite $\mu_{\rm B}$ are obtained using Padé approximant resummations of the quark number susceptibility series. The freeze-out parameters as a function of $\sqrt{s_{\rm NN}}$ are from [41] and $T_{\rm c}$ = 175 MeV.

From comparisons of the experimental data to the HRG model and the lack of non-monotonic dependence of $\kappa\sigma^2$ on $\sqrt{s_{\rm NN}}$ studied, one concludes that there is no indication from the current measurements at RHIC for

a CP in the region of the phase plane with $\mu_B < 200$ MeV. Although it must be noted that the errors on the experimental data point at 19.6 GeV is quite large due to small event statistics. It is difficult to rule out the existence of CP for the entire μ_B region below 200 MeV without the knowledge of the extent of critical region in μ_B. Hence the extent to which these results can do that is guided by the theoretical work. The expectation of the extent of the critical region in μ_B is thought to be about 100 MeV. The results discussed here form the baseline for the future CP search program at RHIC [42]. However the fact that the data shows excellent agreement with HRG and Lattice QCD, both of which assume thermalization, is another non-trivial indication of attainment of thermalization in heavy-ion collisions. Such a conclusion is drawn for the first time using fluctuation measurements. Further the data are compared to lattice QCD calculations for the first time to extract the phase transition temperature to be $T_C \sim 175$ MeV [2].

5. Antimatter discoveries at RHIC

The first ideas of antimatter was proposed in a Nature article by Arthur Schuster titled "Potential Matter A Holiday Dream" in the year 1898. This dream touched upon concepts, which were later realized to be related to matter-antimatter symmetry and validity of CPT theorem. Each of which has now developed into advanced fields of research. It was only in the years 1927-1928, an equation by Paul Dirac predicted a new duality and underlined what Schuster had suggested in 1898. Dirac through his relativistic equation of motion for the electron was able to predict the positron (antimatter partner of the electron), predicted that negative protons must also exist and went on to speculate existence of antimatter stars. Subsequently experiments led to the discovery of positron, antiprotons, antineutrons and antideuteron. In 1995 at CERN, antihydrogen atom was created in LEAR experiment by slowing the antiprotons and attaching positrons. This could lead to test of CPT theorem in near future. On the other hand the realization by Einstein of the equivalence of matter and energy led to the fact that when matter and antimatter meet they annihilate into energy. This fact was used in the Big Bang picture of the Universe to say that the energy was realized into matter and antimatter formation in equal abundance. It led to one of the unsolved problems in science: where did the antimatter of the Universe go? Dedicated search for antimatter nucleus (like anti-α) in space as a reminiscent of the antimatter of the Universe is the main physics motivation of the Alpha Magnetic Spectrometer (called as AMS-02) experiment that has been launched in 2011 to be mounted on the International Space Station.

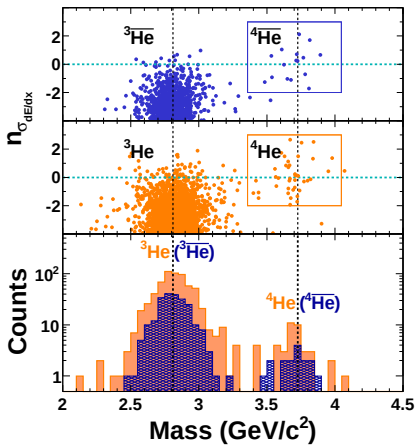

FIG. 5: The top two panels show the ionization energy loss of charged particles in units of multiples of its deviation from theoretical expectations as a function of mass measured by the TOF system. The masses of helium-3 and helium-4 nuclei (and anti-particles) are indicated by the vertical lines at 2.81 GeV/c^2 and 3.73 GeV/c^2, respectively. The bottom panel shows a projection of entries in the upper two panels onto the mass axis.

With timing resolution of 95 pico seconds the STAR Time-Of-Flight (TOF) detector in conjunction with the Time Projection Chamber (TPC) having charged particle energy loss

resolution of better than 8%, allowed to observe 18 candidates of antimatter helium-4 nucleus in the STAR experiment at RHIC [5]. This can be seen from the Mass versus Counts plot and measurement of ionization energy loss using the TOF and TPC in Fig. 5. A detailed systematic estimate of the probability of misidentification of antimatter helium-4 nuclei is of the order of 10^{-11} and possibility of the contribution of background counts to the 18 antimatter helium-4 nuclei is only 1.4 [5]. This discovery has provided a point of reference for possible future observations of antimatter in cosmic radiation and provided rate of production of anti-α in nuclear interactions. The existence of anti-α in space would address one of the major unsolved problem in physics that is understanding precisely how and why there is a predominance of matter over antimatter in the Universe.

A new antinucleus, negatively charged state of antimatter, containing an anti-proton, an anti-neutron, and an anti-Lambda particle was discsovered by STAR experiment in 2010. This is called as the anti-hypertriton. It is also the first anti-nucleus containing an anti-strange quark. All terrestrial nuclei, made of protons and neutrons (which in turn contain only up and down quarks), have a zero value for the quantum number strangeness. The strangeness could be non-zero in the core of collapsed stars, so the present measurements will help us distinguish between models that describe these exotic states of matter.

The anti-hypertriton was identified via its characteristic decay into a light isotope of anti-helium-3 and a positively charged pion. Invariant mass distribution showing the hypertriton and the anti-hypertriton signals over the combinatoric background are shown in the Fig. 5. Altogether, 70 candidates of the anti-hypertriton and 157 hypertritons were found. The measured masses and the life times were about 2. 99 GeV/c^2 and 182 $\pm$ 27 (statistical error) pico seconds for both the nuclei, respectively [4].

This discovery has added a new dimension to the standard periodic table of elements which is arranged according to the number

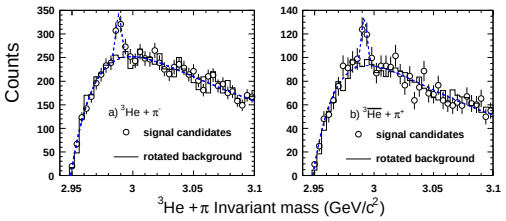

FIG. 6: Left panel: Invariant mass distribution of the daughter helium-3 and pion. Open circles represent the signal candidate distributions, and solid black lines are background distributions. The blue dashed lines are a combination of the signal and background. Right panel: Same for the anti-hypertriton candidate distributions [4].

of protons, which determine each element's chemical properties. We now can have a 3-D chart of the nuclides. In addition to the N-axis corresponding to the number of neutrons, which may change in different isotopes of the same element, the third axis represents strangeness, S, which is zero for all naturally occurring matter. Anti-hypertriton would lie at negative Z and N in such a chart, and the newly discovered anti-strange nucleus would now extends the 3D chart into the new region of strange antimatter. In addition presence of lambda particle in the nucleus can potentially be used to study the properties of the nuclear force in more details. As Lambda has similar mass as the nucleons and can travel deeper inside the nucleus without being subjected to Pauli blocking.

6. Summary and Outlook

RHIC has provided several discoveries to the field of science. We have discovered two new anti-matter nuclei (anti-α and anti-hypertriton). At this facility the high energy heavy-ion collision experiments have seen distinct signatures which suggest that the relevant degrees of freedom in the initial stages of the collisions at 200 GeV are quark and gluons [3]. These signatures includes jet quenching and partonic collectivity are discussed in this paper. The initial temperatures (T_{initial})

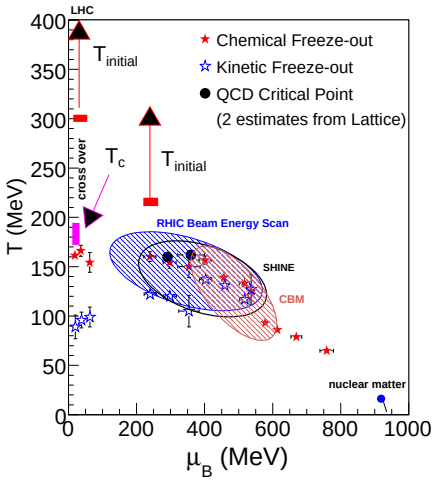

FIG. 7: (Color online) Temperature vs. baryon chemical potential (μ_B) from heavy-ion collisions at various $\sqrt{s_{NN}}$ [42]. The range of critical temperatures (T_c) of the cross-over quark-hadron phase transition at $\mu_B = 0$ [2] and the QCD critical point from two different calculations from lattice QCD are also indicated [43]. Model-based estimates of the range of initial temperature ($T_{\rm initial}$) achieved in heavy-ion collisions based in part on direct photon data at top RHIC [50] and SPS [51] energies are also shown. The range of μ_B to be scanned in the RHIC beam energy scan program corresponding to $\sqrt{s_{NN}} = 5.5$ to 39 GeV as well as experiments at SPS and CBM are indicated as shaded ellipse. The solid point around $T \sim 0$ and $\mu_B = 938$ MeV represents nuclear matter in the ground state.

achieved at top RHIC and SPS energies are obtained from models [52] that explain the direct photon measurements from the PHENIX experiment at RHIC [50] and from the WA98 experiment at SPS [51]. From these models, which assume that thermalization is achieved in the collisions within a time between 0.1–1.2 fm/c, the $T_{\rm initial}$ extracted is greater than 300 MeV at RHIC and greater than 200 MeV at SPS. Further, the understanding of suppression in high p_T hadron production in heavy-ion collisions relative to p+p collisions at RHIC requires a medium energy density $>>$ 1 GeV/fm^3 (critical energy density from lattice for a phase transition). This also shows that the medium has a high degree of opacity to propagation of color charges. In addition the measurement of elliptic flow and the observation of number of constituent quark scaling demonstrates that substantial collectivity has been developed in the partonic phase. The magnitude of the flow across several hadronic species and a small value of viscosity to entropy ratio extracted from the data supports the idea of formation of a strongly coupled system in the heavy-ion collisions. This then also supports the notion of creating a liquid with low viscosity in high energy nuclear collisions [53].

The experiments have also measured the temperature at which the inelastic collisions ceases (chemical freeze-out) and elastic collisions ceases (kinetic freeze-out). These temperatures (as shown in Fig. 7) are extracted from the measured particle ratios and transverse momentum distributions using model calculations which assume the system is in chemical and thermal equilibrium.

New experimental program at RHIC has been designed to explore a large part of the QCD phase digram, covering a μ_B range of 20-600 MeV. Whereas the experimental program at LHC (probing the cross over region of $\mu_B \sim$ 0 MeV of the phase diagram) have started to provide an unique opportunity to understand the properties of matter governed by quark-gluon degrees of freedom at unprecedented high initial temperatures (higher plasma life time) achieved in the Pb+Pb collisions at 2.76-5.5 TeV.

Acknowledgments

This work is supported by DAE-BRNS project Scantion No. 2010/21/15-BRNS/2026.

References

[1] B. Mohanty, New Journal of Physics, **13**, 065031 (2011).
[2] S. Gupta, X. F. Luo, B. Mohanty, H. G. Ritter and N. Xu, Science **332**, 1525 (2011).

[3] STAR Collaboration, J. Adams et al., Nucl. Phys. A **757**, 102 (2005); PHENIX Collaboration, K. Adcox et al., Nucl. Phys. A **757**, 184 (2005).
[4] B. I. Abelev *et al.*, Science **328**, 58 (2010).
[5] H. Agakishiev *et al.*, Nature **473**, 353 (2011).
[6] PHENIX Collaboration, S. S. Adler et al., Phys. Rev. Lett. 91, 072301 (2003); PHOBOS Collaboration, B. B. Back et al., Phys. Rev. Lett. 91, 072302 (2003); STAR Collaboration, J. Adams et al.,Phys. Rev. Lett. 91, 072304 (2003); BRAHMS Collaboration, I. Arsene et al., Phys. Rev. Lett. 91, 072305 (2003).
[7] X.-N. Wang, Miklos Gyulassy, Phys. Rev. Lett. 68, 1480 (1992).
[8] I. Vitev and M. Gyulassy, Phys. Rev. Lett. 89 (2002) 252301; M. Gyulassy, P. Levai,I. Vitev, Phys. Rev. Lett. 85, 5535 (2000).
[9] X-N. Wang, Phys. Rev. C 70, 031901(R) (2004).
[10] M. L. Miller, K. Reygers, S. J. Sanders, P. Steinberg, Ann. Rev. Nucl. Part. Sci. 57, 205 (2007).
[11] STAR Collaboration, B. I. Abelev et al., Phys. Rev. Lett. 97, 152301 (2006); Phys. Lett. B 655, 104 (2007); PHENIX Collaboration, A. Adare et al., arXiv:1004.3532; Phys. Rev. C 82, 011902(R) (2010);Phys. Rev. Lett. 101, 232301 (2008).
[12] S. S. Adler et al., Phys. Rev. Lett. 96, 202301 (2006).
[13] STAR Collaboration, J. Adams et al., Phys. Lett. B 637, 161 (2006).
[14] PHENIX Collaboration, A. Adare et al., Phys. Rev. C 77, 064907 (2008).
[15] PHENIX Collaboration, A. Adare et al., arXiv:1005.1627v2;Phys. Rev. Lett. 98, 172301 (2007).
[16] J. Alam et al., Phys. Rev. D 71 (2005) 094016; arXiv:hep-ph/0604131.
[17] J.-Y. Ollitrault, Phys. Rev. D 46, 229 (1992); H. Sorge, Phys. Rev. Lett.82, 2048 (1999).
[18] S.S. Shi, (for the STAR Collaboration), Nucl. Phys. A 830, 187C (2009).
[19] C. Jena, (for the STAR Collaboration), arXiv:1101.4196 .
[20] D. Teaney, J. Lauret, E. V. Shuryak, Phys. Rev. Lett. 86, 4783 (2001). P. Huovinen, P.F. Kolb, U. Heinz, P.V. Ruuskanen, and S.A. Voloshin, Phys. Lett. B 503, 58 (2001); C. Nonaka et al., Phys. Lett. B 583, 73 (2004). T. Hirano and Y. Nara, Phys. Rev. C 69, 034908 (2004).
[21] STAR Collaboration, J. Adams et al., Phys. Rev. Lett. 92, 052302 (2004); PHENIX Collaboration, S.S. Adler et al., Phys. Rev. Lett. 91, 182301 (2003).
[22] D. Molnar and S.A. Voloshin, Phys. Rev. Lett. 91, 092301 (2003); R. J. Fries et al., Phys. Rev. C 68, 044902 (2003); J.H. Chen et al., Phys. Rev. C 74, 064902 (2006); V. Greco, C.M. Ko, P. Levai,Phys. Rev. Lett. 90, 202302 (2003).
[23] Md. Nasim, et al.,Phys. Rev. C 82, 054908 (2010).
[24] PHENIX Collaboration, A. Adare et al., Phys. Rev. Lett. 98, 162301 (2007); STAR Collaboration, B.I. Abelev et al., arXiv:0909.0566; Phys. Rev. C 77, 054901 (2008).
[25] B. Mohanty and N. Xu, J .Phys. G 36 (2009) 064022 and references therein
[26] Roy A. Lacey et al., Phys. Rev. Lett. 98, 092301 (2007); S. Gavin and M. Abdel-Aziz, Phys. Rev. Lett. 97, 162302 (2006); H-J. Drescher, A. Dumitru, C. Gombeaud, J.-Y. Ollitrault, Phys. Rev. C 76, 024905 (2007).
[27] A. Tang, Nucl. Phys. A 830, 673C (2009).
[28] D. T. Son, A. O. Starinets, Ann. Rev. Nucl. Part. Sci.57, 95 (2007).
[29] L. P. Csernai, J. I. Kapusta, and L. D. McLerran, Phys. Rev. Lett. 97, 152303 (2006).
[30] J. L. Nagle, I. G. Bearden, W, A. Zajc,arXiv:1102.0680.
[31] V. Koch *et al.*, Phys. Rev. Lett. 95, 182301 (2005); M. Asakawa *et al.*, Phys. Rev. Lett. 85, 2072 (2000).
[32] M. A. Stephanov et al., Phys. Rev. D 60, 114028 (1999).
[33] B. Berdnikov et al., Phys. Rev. D 61, 105017 (2000).
[34] M. A. Stephanov, Phys. Rev. Lett. 102, 032301 (2009).

[35] M. Asakawa et al., Phys. Rev. Lett. 103, 262301 (2009).
[36] STAR Collaboration, M. M. Aggarwal et al., Phys. Rev. Lett. 105, 022302 (2010).
[37] R.V. Gavai and S. Gupta, Phys. Lett. B 696, 459 (2011).
[38] F. Karsch and K. Redlich, Phys. Lett. B 695, 136 (2011).
[39] M. Cheng et al., Phys. Rev. D 79, 074505 (2009); B. Stokic et al., Phys. Lett. B 673, 192 (2009).
[40] Y. Hatta *et al.*, Phys. Rev. Lett. **91**, 102003 (2003).
[41] J. Cleymans et al., Phys. Rev. C 73, 034905 (2006).
[42] B. Mohanty, Nucl. Phys. A 830, 899c (2009).
[43] M. Stephanov, Prog. Theor. Phys. Suppl. 153, 139 (2004); Int. J. Mod. Phys. A20, 4387 (2005); Z. Fodor and S.D. Katz, JHEP0404, 50 (2004); R. V. Gavai and S. Gupta, Phys. Rev. D78, 114503(2008); Phys. Rev. D71, 114014 (2005).
[44] STAR Collaboration,J. Adams et al., Phys. Rev. Lett. 98, 062301 (2007); PHENIX Collaboration, A. Adare et al., Phys. Rev. Lett. 98, 232301 (2007).
[45] P. Huovinen, and P.V. Ruuskanen, Ann. Rev. Nucl. Part. Sci. 56, 163 (2006).
[46] Z. Tang et al., arXiv:1101.1912.
[47] E. Schnedermann, J. Sollfrank, and U. Heinz, Phys. Rev. C 48, 2462 (1993).
[48] F. Karsch, Lecture Notes in Physics 583, 209 (2002).
[49] R. Hagedorn, Nuovo Cim. Suppl.3, 147 (1965).
[50] PHENIX Collaboration, A. Adare et al., Phys. Rev. Lett. 104, 132301 (2010).
[51] WA98 Collaboration, M. M. Aggarwal et al., Phys. Rev. Lett. 85, 3595 (2000).
[52] R. Chatterjee, D. K. Srivastava and S. Jeon, Phys. Rev. C 79, 034906 (2009); P. Huovinen, P.V. Ruuskanen and S. S. Rasanen, Phys. Lett. B 535, 109 (2002); A. K. Chaudhuri, J. Phys. G 29, 235 (2003); J. Alam et al., Phys. Rev. C 63, 021901 (2001); D. d'Enterria and D. Peressounko, Eur. Phys. J. C 46, 451 (2006); J. Alam et al., J. Phys. G 34, 871 (2007).
[53] Barbara Jacak and Peter Steinberg, Phys. Today 63N5, 39 (2010).